31P nuclear magnetic resonance titrations: Simultaneous evaluation of all pH-dependent resonance signals

ARTICLE *in* MAGNETIC RESONANCE IN CHEMISTRY · FEBRUARY 1984

Impact Factor: 1.18 · DOI: 10.1002/mrc.1270220209

2 AUTHORS, INCLUDING:

Klaus Dieter Schnackerz
University of Wuerzburg
117 PUBLICATIONS **2,266** CITATIONS

^{31}P Nuclear Magnetic Resonance Titrations: Simultaneous Evaluation of All pH-Dependent Resonance Signals

Heinrich Lachmann*
Physikalisch-chemisches Institut der Universität Würzburg, Marcusstr. 9–11, D-8700 Würzburg, FRG

Klaus D. Schnackerz
Physiologisch-chemisches Institut der Universität Würzburg, Koellikerstr. 2, D-8700 Würzburg, FRG

The simultaneous evaluation of all pH-dependent resonance signals (or multiplets) of an NMR titration offers a substantially increased accuracy and significance. The number of linearly independent titration equilibria is determined by graphical matrix rank analysis. The chemical shifts of all pH-dependent resonance lines are plotted against each other (chemical shift or CS diagrams) indicating whether a single or more titration equilibria are NMR spectrometrically observable and how far they overlap with each other. An iterative curve-fitting program allowing the simultaneous evaluation of all δ(pH) curves is available, from which p*K* values and chemical shifts of all species can be calculated. The starting p*K* values for the iteration need only be estimated very approximately (accuracy ±1–2 units). The titration end-points do not have to be experimentally accessible. The different methods for the simultaneous evaluation of all pH-dependent NMR signals are exemplified in the ^{31}P NMR titration of thiamine pyrophosphate. In this case either the observed resonance lines (two doublets in a broad band proton decoupled spectrum) or the calculated chemical shifts for this AB system can be evaluated. A titration of sodium pyrophosphate was performed and evaluated for comparison.

INTRODUCTION

The methods of simultaneous multiwavelength analysis have recently been developed to a consistent concept which is useful for kinetic analysis of closed or 'open' reaction systems, as well as for the evaluation of spectrometric titration systems. In simultaneous multiwavelength analysis information from a very large spectral range and, perhaps, of different spectrometric techniques (visible–UV absorption, fluorescence, circular dichroism, optical rotatory dispersion, nuclear magnetic resonance, etc.) is correlated for evaluation.

The number of linear independent titration steps in a spectrometric titration is determined by graphical matrix rank analysis.[1–3] This technique was first developed for absorption spectroscopy. The absorbances at two different wavelengths but at the same pH value are plotted against each other (absorbance diagram or A diagram). If only a single titration step is observable over the entire spectral range studied, the A diagrams for any wavelength combination are linear. In more complicated titration systems the so-called absorbance difference quotient diagram, or ADQ diagram, is generally used. Here, quotients of absorption differences at three different wavelengths are plotted against each other, but the same wavelength occupies the denominator ($\Delta A_{\lambda_1}/\Delta A_{\lambda_2}$ versus $\Delta A_{\lambda_3}/\Delta_{\lambda_2}$). The ADQ diagram must be linear for any wavelength combination when two independent titration steps are spectroscopically observable.

Although the methods of graphical matrix rank analysis were initially developed for optical spectroscopy, they can also be easily utilized in non-optical spectroscopy such as NMR or ESR. While in optical spectroscopy the y axis of the spectrum (absorbance, fluorescence intensity, etc.) contains information about the concentrations of different species of a titration system, the analogous information for an NMR titration, at least for a fast-exchanging protolysis equilibrium, is contained in the *x*-axis of the spectrum (ν) or δ). Analogous to A diagrams, the chemical shift diagram or CS diagram was created for NMR titrations, i.e. chemical shifts of different NMR signals obtained at the same pH value are plotted against each other. These diagrams have been used with success for the evaluation of ^{13}C NMR titrations of amino acids and small peptides.[3,4]

When the rank, i.e. the number of linear independent steps of a titration system, is secured by graphical matrix rank analysis, a number of different evaluation techniques can be utilized to determine p*K* values and absorptivities, ε_λ, or δ_0 values of all pure species or ampholytes. For the simultaneous evaluation of all δ(pH) curves an iterative curve-fitting program called TIFIT was successfully applied which was originally developed for absorbance measurements.[5] The iteration can be started with very rough p*K* values (precision ±1–2 pH units). Neither the acid not the alkaline

* Author to whom correspondence should be addressed.

CCC-0030-4921/84/0022-0101$02.50

end-point of the titration has to be quantitatively accessible as a prerequisite for the curve-fitting. The efficiency of the matrix rank analysis and the iterative curve-fitting program will be exemplified on sodium pyrophosphate and thiamine diphosphate.

EXPERIMENTAL

Materials and methods

Fourier transform ^{31}P NMR spectra were recorded at 72.86 MHz on a Bruker WH-180 wide-bore superconducting spectrometer. Sample volumes of 12 ml in 20 mm diameter tubes were used. A concentric 5 mm NMR tube containing ^2H_2O was employed as field/frequency lock. All spectra were recorded with broad band proton decoupling (0.4 W). In general, a 1200 Hz spectral width was acquired in 4096 data points with a 60° pulse angle and 1.7 s repetition time. Continuous air flow through the spectrometer probe head kept the temperature at 20±0.5 °C. Negative chemical shift values indicate resonances at fields higher than the reference, 85% H_3PO_4. The titration was performed in a 50 ml thermostated titration vessel (Metrohm EA 880-50) using a single glass electrode (Metrohm EA 121) connected to a Radiometer pH meter Model PHM 84 and two multiburettes (Metrohm E 485 G5). The pH calibration was performed with four NBS-DIN standard buffers by using linear regression (pH 1.675, 4.002, 6.881 and 9.225 at 20 °C). The titration vessel and the calibration buffers were kept at 20±0.2 °C. After each titration step 12 ml of 0.01 M sodium pyrophosphate or thiamine pyrophosphate containing 1 mM EDTA were transferred to the NMR tube and, after the measurement, returned to the vessel. As titration reagents 1 N HCl or 1 N NaOH were utilized; the latter was kept under N_2 in the burette. The measured δ(pH) values were finally fed into a BASIC computer (Tektronix Model 4052) which serves as a graphic terminal for a large computer (Telefunken Model TR 440) holding the TIFIT program in FORTRAN.

Evaluation methods

Basic equations. For spectrometric acid–base titrations the mixed-mode or apparent dissociation constant is often used instead of the thermodynamic or classical dissociation constant, because the former directly links spectrometrically and electrochemically measurable values. For a one-step protolysis equilibrium

$$BH + H_2O \rightleftharpoons B^- + H_3O^+ \qquad (1)$$

it holds that

$$K = a_{H_3O^+} \cdot \frac{b^-}{bh} \qquad (2)$$

or in logarithmic form

$$pK = pH - \log \frac{b^-}{bh} \qquad (3)$$

where K is the mixed-mode dissociation constant, $a_{H_3O^+}$ the activity of hydronium ions, bh and b^- the molar concentration of BH and B^-, respectively, and the total concentration $b_0 = bh + b^-$. In an NMR titration of a fast one-step protolysis equilibrium, the signal of the observed nucleus shifts between the resonance lines or δ values of the genuine pure species BH and B^-, i.e.

$$\delta = \frac{1}{b_0}(\delta_{BH} \cdot bh + \delta_{B^-} \cdot b^-) \qquad (4)$$

There is an analogous linear connection as for the Beer–Lambert law; instead of the extinction coefficients, ε_λ, the chemical shifts of the pure species are used.

Graphical matrix rank analysis. When one of the concentration variables in Eqn (4) is eliminated, i.e. bh by using the equation $b_0 = bh + b^-$, it follows that

$$\delta = \delta_{BH} + \frac{1}{b_0}(\delta_{B^-} - \delta_{BH})b^- \qquad (5)$$

or

$$\Delta\delta = \delta - \delta_{BH} = \frac{1}{b_0}(\delta_{B^-} - \delta_{BH})b^- \qquad (6)$$

When Eqn (6) is written for two atoms i and j, and both equations are divided by each other, this yields

$$\Delta\delta_i = \frac{\delta_{i_{B^-}} - \delta_{i_{BH}}}{\delta_{j_{B^-}} - \delta_{j_{BH}}} \cdot \Delta\delta_j \qquad (7)$$

Plotting $\Delta\delta_i$ versus $\Delta\delta_j$ for the same pH value results in a straight line starting at the origin (Fig. 1a). In analogous fashion one can derive that the direct plot of δ_i versus δ_j likewise results in a straight line which

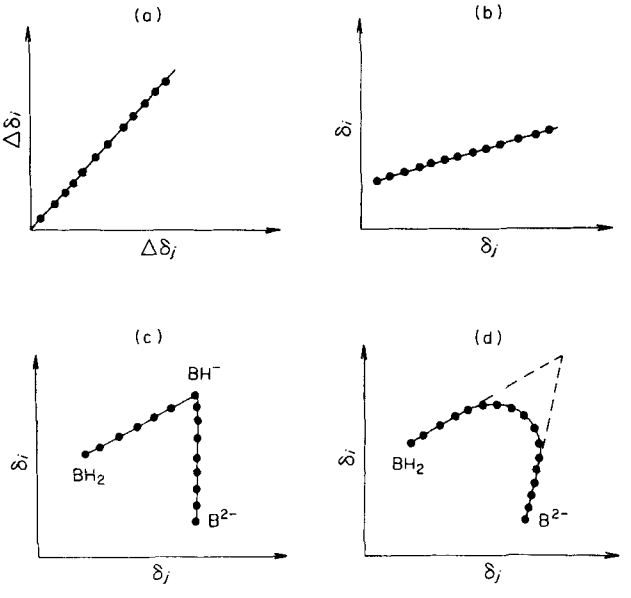

Figure 1. Schematic representation of chemical shift diagrams. (a) Plot of $\Delta\delta_i$ versus $\Delta\delta_j$ according to Eqn (7) for a single-step titration. (b) CS diagram according to Eqn (8) for a single-step titration. (c) CS diagram for a two-step titration with non-overlapping pK values. (d) CS diagram for a two-step titration with overlapping pK values.

does not cross the origin (Fig. 1b):

$$\delta_i = \frac{\delta_{i_{B^-}} - \delta_{i_{BH}}}{\delta_{j_{B^-}} - \delta_{j_{BH}}} \cdot \delta_j + \text{constant} \qquad (8)$$

This diagram is designated as the chemical shift diagram or CS diagram. For a single-step titration system a plot according to Eqns 7 or 8 always results in a straight line.

For a two-step titration ($BH_2 \rightleftharpoons BH^- \rightleftharpoons B^{2-}$) two limiting cases have to be considered.[4]

(a) Non-overlapping titration systems ($\Delta pK > 2.5$–3.0). Such a titration can be formally divided into two one-step partial systems. As shown in Fig. 1c, each CS diagram normally consists of two intersecting straight lines. Their intersection represents the chemical shifts, δ_i and δ_j, of the intermediary species BH^-. The end-points of the straight lines correspond to the pure species BH_2 and B^{2-}, respectively.

(b) Overlapping titration systems ($\Delta pK < 2.5$–3.0). The CS diagrams, shown in Fig. 1d, are usually curved. When tangents are applied to the CS diagrams along the titration end-points BH_2 and B^{2-}, respectively, the intersection of the tangents specify the chemical shifts, δ_i and δ_j, of the intermediary species BH^-. The more the curve deviates from the limiting straight lines in the CS diagram, the more overlap is found in the titration equilibria.

This case will not be discussed in greater detail because it does not apply to any of the examples discussed. The CS diagrams allow statements about the number of titration steps, as well as whether or not there is much overlap in the titration steps.

Determination of pK values. Combining Eqns 3 and 4 results in

$$pK = pH - \log\left(\frac{\delta - \delta_{BH}}{\delta_{B^-} - \delta}\right) \qquad (9)$$

This modified Henderson–Hasselbalch equation is often used for the determination of pK values of single-step NMR titrations. A prerequisite of this methodology is the knowledge of the chemical shifts of the two pure species δ_{BH} and δ_{B^-}, i.e. both titration end-points must be experimentally accessible.

Rearranging Eqn 9 into

$$(\delta - \delta_{BH}) \cdot 10^{-pH} = -K\delta + K\delta_{B^-} \qquad (10a)$$

or

$$(\delta - \delta_{B^-}) \cdot 10^{+pH} = \frac{1}{K}\delta + \frac{1}{K}\delta_{BH} \qquad (10b)$$

yields two additional methods[6,7] for determining the pK value which have rarely been employed for NMR titrations. If one plots the left-hand side of Eqn (10a) or (10b) versus δ one obtains K or $1/K$ from the slope and δ_{B^-} or δ_{BH} from the intercept with the y axis, respectively. In this case it is presumed that only one titration end-point is accessible, whereas the other one can be determined graphically. The linearity of the diagram according to Eqn (10a,b) is simultaneously a criterion of whether the assumed one-step titration mechanism [Eqn (1)] is correct. When Eqn (10) is solved for δ it yields.

$$\delta = \frac{\delta_{BH} \cdot 10^{-pH} + \delta_B K}{10^{-pH} + K} \qquad (11)$$

The correlation between the unknown pK value and the directly measured quantities δ and pH is non-linear. When the function δ(pH) is fitted according to Eqn 11 with an iterative curve-fitting program, only the actual data (δ and pH) enter the calculation. The resonance frequencies of the pure species δ_{BH} or δ_{B^-} do not have to be known, but they can be calculated. In principle, spectrometric titrations can also be evaluated for which both titration end points are not totally accessible.

For the evaluation of the ^{31}P NMR titrations demonstrated below, a FORTRAN curve-fitting program (TIFIT) was used which is specially designed to handle any multistep sequential acid–base titration.[5] For titrations based on absorbance measurements, absorbance time curves A_λ(pH) at different wavelengths (λ_i) can be simultaneously fitted; the fitting program has been used successfully for up to six overlapping and non-overlapping titration steps (H. Lachmann, unpublished results). The fitting program also allows the fitting of δ(pH) curves of different resonance lines simultaneously. The main advantage of this technique is that the total spectral information of a titration can be evaluated synchronously, i.e. δ(pH) curves with relatively small changes in δ can also be assessed. The information contained in different δ(pH) curves supplement each other and thereby allow a particularly precise curve-fitting procedure.

RESULTS AND DISCUSSION

^{31}P NMR titration of thiamine pyrophosphate

The vitamin B_1 derivative thiamine pyrophosphate is an essential cofactor for the oxidative decarboxylation of pyruvate to acetyl coenzyme A, the conversion of glyoxylic acid to tartronic semialdehyde and CO_2 and for the transketolase reaction.[8] α-Hydroxyethyl-thiamine pyrophosphate is a common intermediate in all these reactions.

The broad band proton decoupled ^{31}P NMR spectra of thiamine pyrophosphate show two sharp doublets in the pH range 1–10 which correspond to an AB system (Fig. 2).[9–12] At pH values higher than 8 the pH of the solution drifts towards acidic values for several minutes. For thiamine itself a similar phenomenon has been reported;[13,14] this was interpreted as a slow, reversible opening of the thiazole ring. In the ^{31}P NMR titration curves shown in Fig. 2 this drift is hardly recognized, since the δ values are practically constant at pH values above 8. For this reason this phenomenon has apparently not been observed in other studies.[9–12] A comprehensive kinetic spectrometric study of thiamine pyrophosphate is currently in progress. At pH values lower than 1 a slight time-dependent shift of the pH value is observed.

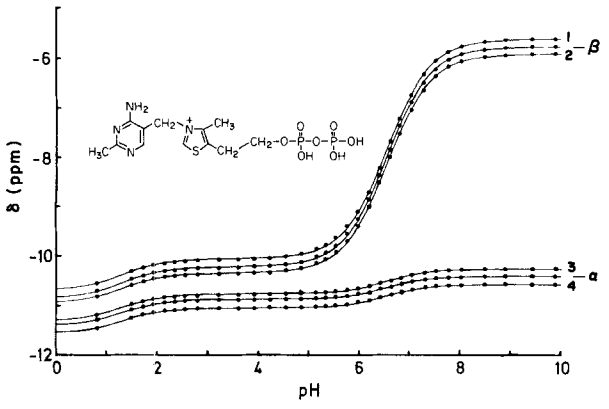

Figure 2. δ(pH) data of thiamine pyrophosphate simulated with the TIFIT program: 1–4, recorded resonance lines of both doublets; α,β, chemical shifts calculated for an AB system. The solid lines represent the simulation.

Therefore, the first two dissociation steps of the pyrophosphate (pK_1, pK_2) were not accurately established. Here we have a case in which both titration end-points are difficult to reach experimentally, or in which the substance changes at extreme pH values.

Figure 2 shows the pH dependence of the four resonance lines of the chemical shifts δ_α and δ_β, respectively. The coupling constant $J(\alpha\beta)$ changes very little with pH (20.5 Hz at pH 2, 22.5 Hz at pH 8[9]). At pH 10 $J(\alpha\beta)$ is small compared with the distance $\Delta\delta$ between the two doublets; at pH < 4, however, $J(\alpha\beta)$ and $\Delta\delta$ are of comparable magnitude ($J/\Delta\delta \approx 2/1$ at pH 2). Therefore, all four resonance lines were used to calculate the chemical shifts δ_α and δ_β in the AB system; these are also shown in Fig. 2. At pH > 8 the chemical shift corresponds to the mean of the doublet, i.e. weak coupling, whereas at pH < 5 the chemical shifts are shifted to the centre of both doublets owing to the stronger coupling. By combining the four observed curves in Fig. 2 in a CS diagram (Fig. 3a and b) the following observations can be made. On plotting the chemical shifts of the same doublet against each other a straight line results over the entire pH range. Neither CS diagrams contain any information about the number of titration steps. This is true when the coupling constant $J(\alpha\beta)$ is independent of pH, i.e. $\nu_1(\text{pH}) = \nu_2(\text{pH}) + J$. The small pH dependence of $J(\alpha\beta)$ of the order of 1–2 Hz is invisible on the ppm scale of the CS diagram. Plotting the δ(pH) curves of different doublets against each other results in two intersecting straight lines in the CS diagram, i.e. a non-overlapping two-step titration system according to Fig. 1c.

An additional dissociation step of the pyrophosphate (pK_1) cannot be recognized in the ^{31}P NMR spectra at pH > 0.5. When the chemical shifts δ_α and δ_β calculated for an AB system (Fig. 2) are plotted against each other in a CS diagram (Fig. 3c), two intersecting straight lines are again obtained. Therefore, it can be concluded from the CS diagram that in the pH range 1–10 two non-overlapping titration steps can be observed in the ^{31}P NMR spectra of thiamine pyrophosphate. The δ(pH) curves can be evaluated either as a two-step titration or can be divided into

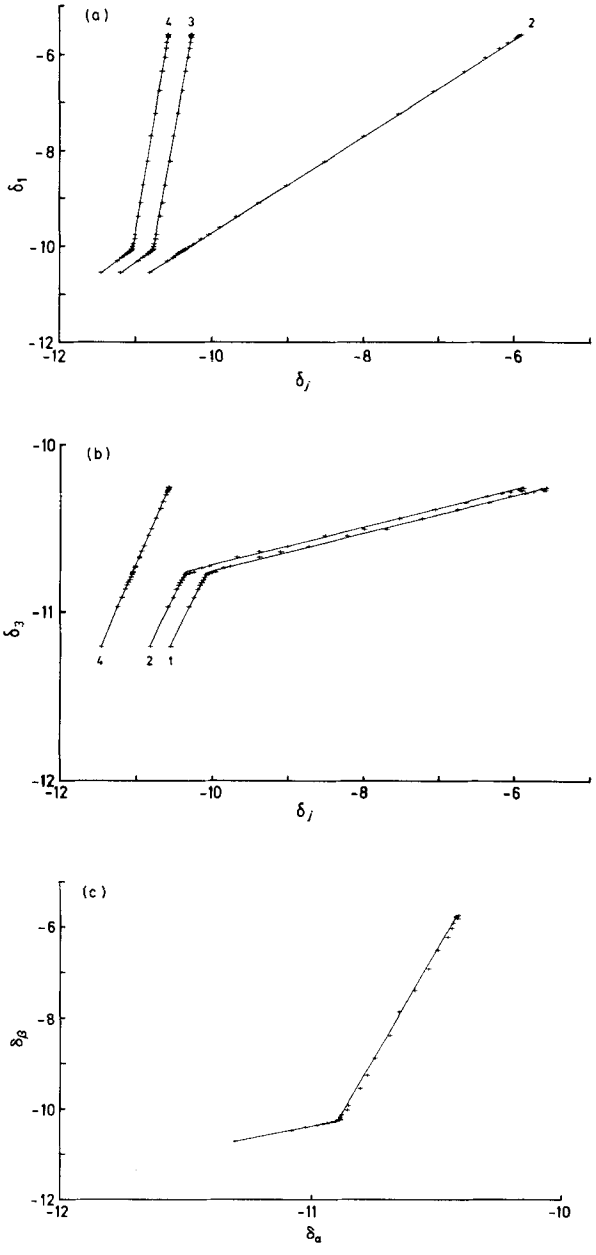

Figure 3. CS diagrams of the measured resonance lines 1–4 of both doublets. (a) Resonance line 1 is the reference on the ordinate; (b) resonance line 3 is the reference on the ordinate. (c) CS diagram of the calculated chemical shifts δ_α versus δ_β.

two single-step partial titrations. The iterative curve-fitting program TIFIT can handle these data both ways with the same results.

Since the coupling is relatively weak in the pH range 1–4 ($J/\Delta\delta > 1$) the measured resonance lines 1–4, as well as δ_α(pH) and δ_β(pH) can be used for evaluation. The most accurate and significant results are obtained when all experimental data are evaluated simultaneously as a two-step titration (either lines 1–4 or δ_α and δ_β). A simultaneous evaluation of all six curves would be statistically not agreeable because δ_α and δ_β are derived mathematically from the remaining four curves.

The calculated mixed-mode pK values are $pK_2 = 1.35 \pm 0.1$ and $pK_3 = 6.57 \pm 0.01$. For the evaluation of

pK_2 only a few data points and, among them, only one below the pK_2 value, were available. Omission of one or two data points at the acidic end of the titration changes the calculated pK_2 value distinctly. Omitting 3–4 data points at the alkaline end of the titration does not affect the evaluation of the pK_3 value. The pK_3 value is therefore much more reliable than the pK_2 value. The reported pK_3 values[9,11] are in the range 6.5–6.7. The chemical shifts of the separate species calculated according to the TIFIT program are listed in Table 1.

Table 1. Chemical shifts of the separate species in thiamine pyrophosphate

	BH_2	BH^-	B^{2-}
δ_α (ppm)	−11.41	−10.87	−10.40
δ_β (ppm)	−10.86	−10.21	−5.75

The solid lines in Fig. 2 represent a simulation using the above stated pK values and the δ values of all species (BH_2, BH^-, B^{2-}), respectively, from the TIFIT program. Experimentally observed data points are in very good agreement with the simulated curves.

^{31}P NMR titration of pyrophosphoric acid

For comparison, pure pyrophosphoric acid was titrated. The pH-dependent ^{31}P NMR spectra show a single resonance signal, because both phosphorus nuclei are magnetically equivalent (A_2 system).[15] CS diagrams are therefore not possible. Figure 4 demonstrates the pH dependence of the chemical shift of pyrophosphate. The dissociations of the first two protons (i.e. pK_1 and pK_2) were not determined. Only data obtained at pH>3 were evaluated as a two-step titration system. The TIFIT program allowed the calculation of $pK_3 = 6.25 \pm 0.01$ and $pK_4 = 8.64 \pm 0.01$. The pyrosphosphate system is a weak overlapping titration system ($\Delta pK = 2.39$). The published pK values[16,17] vary between 5.8 (18 °C) and 6.6 (25 °C) for pK_3 and between 8.2 (18 °C) and 9.3 (25 °C) for pK_4, respectively. The chemical shifts of the pure species BH_2, BH^- and B^{2-}, calculated according to the TIFIT program, are −10.01, −6.89 and −5.93 ppm, respectively.

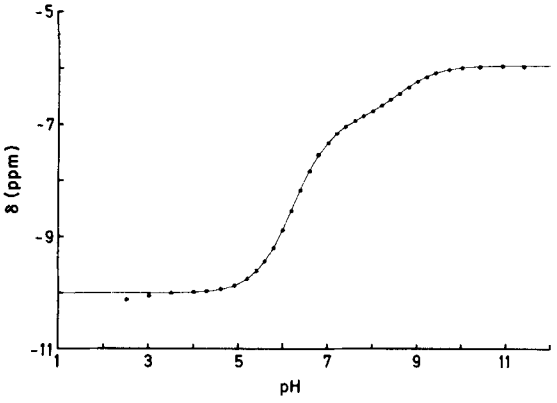

Figure 4. δ(pH) data for sodium pyrophosphate (●) and a simulation according to the TIFIT program (—).

The solid line in Fig. 4 corresponds to a simulation with the above-stated pK values and the δ values, which shows an excellent fit at pH>3.

CONCLUSIONS

The simultaneous evaluation of the δ(pH) curves of several atoms, or of all resonance lines created by spin–spin coupling, allows the possibility of a very accurate and significant analysis of NMR titrations. If, as in the case of pyrophosphoric acid, only a single δ(pH) curve exists, the evaluation by graphical matrix rank analysis using CS diagrams is not possible.

The iterative curve-fitting program, however, is independent of CS diagrams. It offers the possibility of evaluating either single titration steps or all δ(pH) curves simultaneously. Thereby it is irrelevant whether, and how far, different titration steps overlap. There is no prerequisite for the acidic or alkaline end of the titration curve to be experimentally accessible. A systematic study on how much information at the titration ends can be missing is currently in progress.

REFERENCES

1. H. Lachmann, H. Mauser and F. Schneider, *Z. Naturforsch., Teil B* **29**, 500 (1974).
2. R. Blume, H. Lachmann and J. Polster, *Z. Naturforsch., Teil B* **30**, 263 (1975).
3. H. Lachmann, *Z. Anal. Chem.* **290**, 117 (1978).
4. D. Leibfritz, E. Haupt, N. Dubischar, H. Lachmann, R. Oekonomopulos and G. Jung, *Tetrahedron* **38**, 2165 (1982).
5. F. Göbber and H. Lachmann, *Z. Physiol. Chem.* **359**, 269 (1978).
6. J. H. Baxendale and H. R. Hardy, *Trans. Faraday Soc.* **49**, 1140 (1953).
7. V. Böhmer, R. Wamsser and H. Kämmerer, *Monatsh. Chem.* **104**, 1315 (1973).
8. L. O. Krampitz, *Annu. Rev. Biochem.* **38**, 213 (1969).
9. A. M. Chauvet-Monges, M. Hadida, A. Crevat and E. J. Vincent, *Arch. Biochem. Biophys.* **207**, 311 (1981).
10. A. M. Chauvet-Monges, M. Hadida and A. Crevat, *C.R. Acad. Sci., Ser. C* **286**, 489 (1978).
11. J. P. Taglioni and J. Fournier, *C.R. Acad. Sci., Ser. C* **288**, 141 (1979).
12. D. R. Petzold and W. Storek, *Stud. Biophys.* **75**, 1 (1979).
13. D. E. Metzler, in *The Enzymes*, edited by P. D. Boyer, H. Lardy and K. Myrbäck, Vol. 2, p. 295. (1960).
14. T. C. Bruice and S. J. Benkovic, *Bioorganic Mechanisms*, Vol. II, pp. 204. W. A. Benjamin, New York (1966).
15. M. M. Crutchfield, C. H. Dungan and J. R. van Wazer, in *Topics in Phosphorus Chemistry*, edited by H. Grayson and E. J. Griffiths, Vol. 5. Interscience, New York, (1967).
16. H. A. Sober (Ed.), 2nd ed. Handbook of Biochemistry, Chemical Rubber Co., Cleveland, Ohio (1970).
17. R. C. Weast (Ed.), *Handbook of Chemistry and Physics*, 59th ed. CRC Press, Boca Raton (1979).

Received 1 July 1983; accepted 27 July 1983